Bull. Malays. Math. Sci. Soc. (2025) 48:53
https://doi.org/10.1007/s40840-025-01827-3

BULLETIN *of the*
MALAYSIAN MATHEMATICAL
SCIENCES SOCIETY
http://www.springer.com/mathematics/journal/40840

A Mechanistic Model-to-Model Approach for Solving a Nonlinear Pharmacokinetic Model

Xiaotian Wu[1] · Weimiao Zhang[1] · Xiang-Sheng Wang[2] · Jun Li[3,4]

Received: 29 August 2024 / Revised: 4 January 2025 / Accepted: 12 January 2025

Abstract

The mathematical solution for drug concentration over time is a cornerstone of quantitative pharmacology, forming the foundation for optimizing drug use to ensure both efficacy and safety. In this study, we investigated the explicit expression of drug concentration over time in a one-compartment pharmacokinetic model with simultaneous first-order and Michaelis-Menten elimination under first-order oral absorption-an open problem in the literature. To address this, we introduce a novel model-to-model approximate approach that enables the analytical expression of drug concentration over time with any desired precision. The developed approximation consists of a sequence of pharmacokinetic sub-models, each possessing a known analytical solution. Notably, these sub-models retain key pharmacokinetic properties, such as distribution, elimination, and total administered dosage. The proposed method is validated through rigorous mathematical proofs and numerical simulations. Compared to existing methods, our approach is more direct and efficient, specifically preserving the mechanistic pharmacology of drug fate while requiring only a small sample size to achieve controllable precision. These findings pave the way for novel advancements in the analysis of pharmacokinetic models, with significant implications for optimizing drug therapy.

Keywords Mathematical pharmacology · Simultaneous first-order and Michaelis-Menten elimination · First-order absorption · Mechanistic model-to-model approximation · Explicit solution

Mathematics Subject Classification 92C45 · 34A45 · 65H99

Communicated by Rosihan M. Ali.

✉ Jun Li
jun.li.2@umontreal.ca

1 School of Science, Shanghai Maritime University, Shanghai 201306, People's Republic of China

2 Department of Mathematics, University of Louisiana at Lafayette, Lafayette, LA 70503, USA

3 Faculté de pharmacie, Université de Montréal, Montréal, Québec H3C 3J7, Canada

4 Centre de recherches mathématiques, Université de Montréal, Montréal, Québec H3C 3J7, Canada

Published online: 19 February 2025

1 Introduction

Pharmacokinetic (PK) modelling is a crucial aspect of quantitative pharmacology. The ability to analytically express the solution of a PK model, namely, drug concentration as a function of time ($C(t)$), is essential to understand drug properties and provid the theoretical foundation for optimizing drug use in terms of efficacy and safety [1–7]. However, with significant evidence of nonlinearity found in drug mechanisms, nonlinear features have become a major concern in current PK modelling. This introduces substantial challenges, making it difficult or even impossible to find analytical solutions using conventional elementary functions. As a result, the use of transcendental functions has been proposed and increasingly applied. A well-known example is the one-compartment PK model with the nonlinear Michaelis-Menten elimination under intravenous (IV) bolus or constant infusion, where the transcendental Lambert W function is repeatedly discovered to express the solution of $C(t)$ [8]. Another example involves the fractional PK models, where the Mittag-Leffler function is found the application in the expression of their analytical solutions [7, 9]. Additionally, there are specific analyses of saturable absorption models, where analytical solutions using elementary, Lambert W and Wright functions have been established for drug absorption process of the Hill kinetic type [10].

In the current paper, we are interested in the simultaneous linear and Michaelis-Menten elimination. This type of nonlinear elimination has been widely reported for biologics, such as hormones, growth factors, monoclonal antibodies [11, 12]. In this scenario, the drug substance is eliminated from the body, represented by the drug concentration, at the rate:

$$\frac{dC(t)}{dt} = -k_{el}C(t) - \frac{V_{max}C(t)}{K_m + C(t)}, \tag{1}$$

where the first term on the right side represents a linear elimination pathway with a rate constant k_{el}, and the second term on the right side is a nonlinear saturate elimination pathway characterized by Michaelis-Menten kinetics with a maximum elimination rate V_{max} and Michaelis constant K_m. The nonlinearity induced by the nonlinear elimination described in Model (1) makes it mathematically challenging to find the analytical solution for $C(t)$. Although numerical solutions can be applied in PK practices, an accurate symbolic mathematical relationship is always preferred for better understanding and delineation of the mechanism underlying the model. Following this logic, we have studied PK as described by Model (1) and established analytical solutions for $C(t)$ in the cases of IV bolus and constant infusion by introducing new transcendental X and Y functions, respectively [13, 14].

A convenient way of drug administration facilitates better control of drug disposition, the route of administration is the crucial factor in shaping the absorption aspect of a drug. Various pharmaceutical formulations exist (e.g., liquids, capsules, tablets, or chewable tablets), with oral or other controlled-release medications being the most popular due to their convenience, safety, and cost-effectiveness [15, 16]. Typically, the first-order kinetics, proportional to the drug amount at the absorption site, is assumed

for oral drugs to describe their systemic absorption into plasma circulation. Mathematically, a one-compartment PK model with simultaneous linear and Michaelis-Menten elimination for the first-order absorption after a single dose D can be described as:

$$\begin{cases} \dfrac{dA_a(t)}{dt} = -k_a A_a(t), \quad t > 0, \\ \dfrac{dC(t)}{dt} = \dfrac{Fk_a A_a(t)}{V_d} - k_{el}C(t) - \dfrac{V_{max}C(t)}{K_m + C(t)}, \quad t > 0, \\ A_a(0^+) = D, \quad C(0) = 0, \end{cases} \tag{2}$$

where $A_a(t)$ is the amount of drug available for absorption into the systemic circulation at time t, k_a is the absorption rate constant, and F is the bioavailability, representing the fraction of the dose absorbed into the systemic circulation.

In fact, we have $A_a(t) = A_a(0^+)e^{-k_a t} = De^{-k_a t}$, and we can simplify Model (2) into the following one-compartment PK model with the first-order absorption:

$$\begin{cases} \dfrac{dC(t)}{dt} = \dfrac{FD}{V_d}k_a e^{-k_a t} - k_{el}C(t) - \dfrac{V_{max}C(t)}{K_m + C(t)}, \quad t > 0, \\ C(0) = 0. \end{cases} \tag{3}$$

As we can see in Model (3), the time-varying absorption and parallel elimination processes are nonlinearly intertwined and not separable, and the nonlinear differential equation is non-autonomous, making it impossible to transform into an algebraic equation. Instead, an alternative analytical expression to approximate the exact solution is desirable for problem-solving. Thus, we propose to develop a mechanistic model-to-model approach that provides analytical solutions capable of approximating and converging to the exact $C(t)$ while *preserving the drug's partial PK properties*. Since we have already established the analytical solutions of PK Model (1) for the drug administration routes of IV bolus and constant infusion using transcendental X and Y functions, we will apply these results to approximate the exact solution of Model (3). Therefore, these mathematical results will have a direct impact on applications in the drug-controlled release, whether for new formulation design or precise clinical drug use [17]. However, as we will observe below, the obtained mathematical results are neither straightforward nor simple, which poses challenges for readers seeking a deep understanding of both mathematics and pharmacology.

This paper is organized as follows. In Sect. 2, we review the current knowledge on analytical solutions of Model (1) for the cases of IV bolus and constant infusion administrations. In Sect. 3, we present how to obtain analytical solutions that converge to and approximate the exact solution of Model (3) using previously studied PK models. In Sect. 4, we provide a theoretical proof of the relationship between the proposed analytical solutions of the involved PK models and the exact solution of Model (3). In Sect. 5, simulations are performed to demonstrate the robustness of the proposed approach. The paper concludes with a brief discussion and conclusion.

2 Current Knowledge for the Intravenous Bolus and Constant Infusion Administrations

In this section, we will review the results of Model (1) for both IV bolus and constant infusion administrations. These solutions will serve as the basis for developing the explicit expressions of Model (3).

2.1 Intravenous Bolus

If a single dose D is administered by IV bolus at time t_0, then the PK model with simultaneous first-order and Michaelis-Menten elimination is

$$\begin{cases} \dfrac{dC(t)}{dt} = -k_{el}C(t) - \dfrac{V_{max}C(t)}{K_m + C(t)}, & t > t_0 \\ C(t_0^+) = \frac{D}{V_d} \triangleq C_0, & t = t_0, \end{cases} \tag{4}$$

where C_0 is the initial concentration immediately after the IV bolus administration. In order to have its solution $C(t)$, we introduce the following transcendental X function.

Definition 1 [13] For $s \in \mathbb{R}$, $X(s, p_1, p_2)$ is defined as the multi-valued solution of the following equation

$$\Big(X(s, p_1, p_2)\Big)^{p_1}\Big(1 + X(s, p_1, p_2)\Big)^{p_2} = s, \tag{5}$$

where p_1 and p_2 are given positive real constants.

Based on the above definition of X function, the solution of Model (4) is

$$C(t) = C_\beta \times X_0\left(\left(\frac{C_0}{C_\beta}\right)^{p_1}\left(1 + \frac{C_0}{C_\beta}\right)^{p_2} e^{-k_{el}(t-t_0)}, p_1, p_2\right),$$

where

$$p_1 = \frac{k_{el}}{k_{el} + k_{em}}, \quad p_2 = \frac{k_{em}}{k_{el} + k_{em}} \quad \text{and} \quad C_\beta = K_m\frac{k_{el} + k_{em}}{k_{el}}. \tag{6}$$

Here $k_{em} = V_{max}/K_m$ and $p_1 + p_2 = 1$, and X_0 is the principal real branch of X function that has been previously investigated in [18].

2.2 Constant Infusion

In the case of constant infusion, the PK model with the simultaneous fist-order and Michaelis-Menten elimination is

$$\begin{cases} \dfrac{dC(t)}{dt} = r - k_{el}C(t) - \dfrac{V_{max}C(t)}{K_m + C(t)}, & t > t_0, \\ C(t_0) \triangleq C_0 \geq 0, & t = t_0, \end{cases} \tag{7}$$

where r is the infusion rate and C_0 is the drug concentration at the infusion starting time t_0. Model (7) admits a unique positive equilibrium

$$C^{\infty} = \frac{1}{2}\left[\sqrt{\left(C_\beta - \frac{r}{k_{el}}\right)^2 + 4\frac{r}{k_{el}}K_m} - \left(C_\beta - \frac{r}{k_{el}}\right)\right] \tag{8}$$

with the notation C_β introduced in Eq. (6). It is noteworthy that C^{∞} is r-dependent and globally asymptotically stable for any initial concentration $C_0 \geq 0$ [14].

In order to obtain the expression of $C(t)$ of Model (2), the following parameters derived from model parameters are required

$$\begin{aligned} q_1 &= \frac{C^{\infty} + K_m}{C^{\infty} + C_\beta^{\infty}} > 0,\ q_2 = \frac{C_\beta^{\infty} - K_m}{C^{\infty} + C_\beta^{\infty}} > 0, \\ C_\beta^{\infty} &= \frac{1}{2}\left[\sqrt{\left(C_\beta - \frac{r}{k_{el}}\right)^2 + 4\frac{r}{k_{el}}K_m} + \left(C_\beta - \frac{r}{k_{el}}\right)\right] > 0, \end{aligned} \tag{9}$$

with $q_1 + q_2 = 1$. Then, we introduce the following transcendental Y function [14].

Definition 2 [14] For $s \in \mathbb{R}$, $Y(s, q_1, q_2)$ is defined as the multi-valued solution of the following equation

$$\Big(Y(s, q_1, q_2)\Big)^{q_1}\Big(1 - Y(s, q_1, q_2)\Big)^{q_2} = s, \tag{10}$$

where q_1 and q_2 are given positive real constants.

With the transcendental Y function, the analytical solution of Model (7) is possible, which depends on the relationship between C_0 and C^{∞}. We summarize the results below.

Theorem 1 *[14] For Model (7), the solution of drug concentration $C(t)$ can be one of the following situations:*

1. *If $C_0 < C^{\infty}$, $C(t)$ displays the upward trend and converges to the equilibrium concentration C^{∞} as $t \to \infty$. Moreover, $C(t)$ can be explicitly expressed as*

$$C(t) = C^{\infty} - (C^{\infty} + C_\beta^{\infty}) \times Y_0\left(\left(\frac{C^{\infty} - C_0}{C^{\infty} + C_\beta^{\infty}}\right)^{q_1}\left(\frac{C_0 + C_\beta^{\infty}}{C^{\infty} + C_\beta^{\infty}}\right)^{q_2} e^{-k_{el}(t - t_0)}, q_1, q_2\right), \tag{11}$$

   where Y_0 is the principal real branch of Y function.
2. *If $C_0 = C^{\infty}$, $C(t) = C_0$ for all $t \geq t_0$;*
3. *If $C_0 > C^{\infty}$, $C(t)$ displays the downward trend and converges to the equilibrium concentration C^{∞} as $t \to \infty$. Moreover, $C(t)$ can be explicitly expressed as*

$$C(t)=C^{\infty}+(C^{\infty}+C_{\beta}^{\infty})\times X_0\left(\left(\frac{C_0-C^{\infty}}{C^{\infty}+C_{\beta}^{\infty}}\right)^{q_1}\left(\frac{C_0+C_{\beta}^{\infty}}{C^{\infty}+C_{\beta}^{\infty}}\right)^{q_2}e^{-k_{el}(t-t_0)},q_1,q_2\right), \tag{12}$$

where X_0 is the principal real branch of X function.

3 Design of Mechanistic PK Sub-Models with Constant Infusion

For Model (3), it can be observed that

$$r_{1,i}\triangleq\frac{FD}{V_d}k_a e^{-k_a t_{i+1}}\le\frac{FD}{V_d}k_a e^{-k_a t}\le\frac{FD}{V_d}k_a e^{-k_a t_i}\triangleq r_{2,i} \tag{13}$$

for any $t\in[t_i,t_{i+1}]$. By inputting the constant infusion rates $r_{1,i}$ and $r_{2,i}$ into Model (7) restricted to the subinterval $[t_i,t_{i+1}]$, we can derive the local and global upper and lower bounds of drug concentration over time by using the comparison theorem of differential equations, thus forming an approximate solution to Model (3) within the specified bounds. However, this approximation lacks pharmacological utility in clinical practice because selecting the appropriate infusion rates $r_{1,i}$ and $r_{2,i}$ is challenging. Furthermore, achieving a satisfactory approximation requires dividing the time interval with a large number of points, which is impractical in clinical applications. To address these limitations and enable a more efficient and clinically applicable solution, we will develop a novel methodology for solving Model (3). This approach will not only be mathematically tractable but also preserve pharmacological relevance.

Suppose we have sampled drug concentrations, C_{0s}, C_{1s}, C_{2s}, $\cdots$, C_{ns}, as raised by the PK oral Model (3), on their corresponding sampling time points, $T_0<T_1<T_2<\cdots<T_n$, which are chosen in an increasing manner. Furthermore, in a deterministic fashion, we assume there is no residual error, i.e., $C_{is}=C(T_i)$ for $i=0,1,\cdots,n$, and, in particular, $C_{0s}=0$ at $T_0=0$.

On each $[T_i,T_{i+1}]$, we suggest to replace the time-varying drug input of Model (3) with a constant infusion process while not altering the dose amount absorbed therein, hence the dose amount absorbed is

$$D_i=\int_{T_i}^{T_{i+1}}FDk_a e^{-k_a t}\,dt=FD\left(e^{-k_a T_i}-e^{-k_a T_{i+1}}\right).$$

This leads to a constant infusion rate in $[T_i,T_{i+1}]$ as

$$r_i=\frac{D_i}{T_{i+1}-T_i}\Big/V_d=\frac{FD}{V_d}\frac{e^{-k_a T_i}-e^{-k_a T_{i+1}}}{T_{i+1}-T_i}=\frac{FD}{V_d}k_a e^{-k_a\xi_i}, \tag{14}$$

for some $\xi_i\in(T_i,T_{i+1})$ by the Lagrange mean value theorem. Accordingly, we obtain a sequence of new PK models by substituting the time-varying input rate of Model (3)

with the time-invariant constant input rate $\frac{FD}{V_d}k_a e^{-k_a\xi_i}$, *i.e.*,

$$\begin{cases} \dfrac{d\tilde{C}_i(t)}{dt} = \dfrac{FD}{V_d}k_a e^{-k_a\xi_i} - k_{el}\tilde{C}_i(t) - \dfrac{V_{max}\tilde{C}_i(t)}{K_m + \tilde{C}_i(t)}, \quad t \in (T_i, T_{i+1}], \\ \tilde{C}_i(T_i) = C(T_i) = C_{is}, \end{cases} \tag{15}$$

for $i = 0, 1, 2, \cdots$. Note that the analytical solution of $\tilde{C}_i(t)$ of above model can be given as shown in Theorem 1.

Furthermore, for the sake of mathematical rigour, we assume $\tilde{C}_i(t) = 0$ for $t \notin [T_i, T_{i+1}]$. Adding all solutions of PK sub-models (15) yields a solution consisting of piecewise analytical expressions:

$$\tilde{C}(t) = \sum_{i\in\{1,2,\cdots,n\}} \tilde{C}_i(t), \tag{16}$$

which approximates the exact solution of the oral PK Model (3) with the same absorbed dose.

In the following, we will demonstrate that $\tilde{C}(t)$ in Eq. (16) can effectively approximate $C(t)$ in Model (3), both theoretically and numerically.

4 Theoretical Results

First, for PK Model (3), we have the following mathematical properties.

Lemma 1 *Denote* $f(t) = \frac{FD}{V_d}k_a e^{-k_a t}$ *for* $t > 0$ *and* $g(x) = k_{el}x + \frac{V_{max}x}{K_m+x}$ *for* $x > 0$, *we have:*

$$f(t) > 0,\ f'(t) < 0,\ f''(t) > 0,\ f(t)f''(t) = [f'(t)]^2, \tag{17}$$

$$g(x) > 0,\ g'(x) > 0,\ g''(x) < 0,\ g'''(x) > 0. \tag{18}$$

Proof The proof of the above properties is direct. □

To ensure that $\tilde{C}(t)$ can effectively approximate $C(t)$, the error of this approximation should to be analyzed. To do this, we first clarify the shape behaviours of $C'(t)$ and $\tilde{C}_i{}'(t)$ with the aim to analyze the intersection point of $C'(t)$ and $\tilde{C}_i{}'(t)$.

Lemma 2 *For the oral Model (3) and proposed PK sub-models (15), we have*

(i) There exists t_{max} *and* t^* *with* $t^* > t_{max}$ *such that*

$$C'(t_{max}) = 0,\ C'(t) > 0 \text{ for } t \in [0, t_{max}), C'(t) < 0 \text{ for } t \in (t_{max}, \infty), \lim_{t\to\infty} C'(t) = 0; \tag{19}$$

$$C''(t^*) = 0,\ C''(t) < 0 \text{ for } t \in [0, t^*), C''(t) > 0 \text{ for } t \in (t^*, \infty); \tag{20}$$

(ii) If $\tilde{C}_i{}'(T_i) > 0$, *then* $\tilde{C}_i{}'(t) > 0$, $\tilde{C}_i{}''(t) < 0$ *and* $\tilde{C}_i{}'''(t) > 0$ *for* $t \in (T_i, T_{i+1})$. *If* $\tilde{C}_i{}'(T_i) < 0$, *then* $\tilde{C}_i{}'(t) < 0$ *and* $\tilde{C}_i{}''(t) > 0$ *for* $t \in (T_i, T_{i+1})$.

Proof The proof is standard. □

Lemma 3 *Consider* $E_i(t) = \tilde{C}_i(t) - C(t)$, *which is the piecewise approximation error of Model (15) to Model (3) during each subinterval* (T_i, T_{i+1}), *there exists a unique time point* $S_i^* \in (T_i, \xi_i)$ *such that* $E_i(S_i^*)$ *is a local minimum and* $E_i'(S_i^*) = 0$.

Proof *(a)* First, we show there exists a time point $S_i^* \in (T_i, \xi_i)$ such that $E_i(S_i^*)$ is a local minimum.

Using the Comparison Theorem for Model (3) and Model (15), we have $C(t) > \tilde{C}_i(t)$ for $t \in (T_i, \xi_i]$, and particularly, it is noteworthy that $C(\xi_i) > \tilde{C}_i(\xi_i)$. On the one hand, we have $E_i'(T_i) = f(\xi_i) - f(T_i) < 0$ since $f'(t) < 0$ and $\xi_i > T_i$, but on the other hand, we have $E_i'(\xi_i) = g(C(\xi_i)) - g(\tilde{C}_i(\xi_i)) > 0$ since $g'(x) > 0$ and $C(\xi_i) > \tilde{C}_i(\xi_i)$. By Intermediate Zero Theorem, there exists at least a $S_i^* \in (T_i, \xi_i)$ such that $E_i'(S_i^*) = 0$ and $E_i(S_i^*)$ is a local minimum.

(b) Second, we show the uniqueness of S_i^* in terms of three scenarios: $\tilde{C}_i{}'(T_i) = 0$, $\tilde{C}_i{}'(T_i) < 0$ and $\tilde{C}_i{}'(T_i) > 0$.

(i) If $\tilde{C}_i{}'(T_i) = 0$, we have $\tilde{C}_i{}'(t) = 0$ for all $t \in (T_i, \xi_i]$, which is directly resulted from the dynamics of Model (15). Meanwhile, as $C'(T_i) = f(T_i) - g(C(T_i)) > f(\xi_i) - g(\tilde{C}_i(T_i)) = 0$, which implies there is a unique $t_1 \in (T_i, \xi_i)$ such that $\tilde{C}_i{}'(t_1) = C'(t_1)$ by Lemma 2. In fact, $t_1 = S_i^*$ by *(a)*.

(ii) If $\tilde{C}_i{}'(T_i) < 0$, then $\tilde{C}_i{}'(t) < 0$ for all $t \in [T_i, \xi_i]$ by Lemma 2. The uniqueness of zero of $E_i'(t)$ for $t \in (T_i, \xi_i)$ can be shown using proof by contradiction. Assume $t_1 < t_2$ are two consecutive zero points of $E_i'(t)$ in (T_i, ξ_i). Then, we have $C'(t_k) = \tilde{C}_i{}'(t_k)$, $\tilde{C}_i{}'(t_k) < 0$ as well as $C(t_k) > \tilde{C}_i(t_k)$, $k = 1, 2$. By Lemma 1, we have $f'(t) < 0$, $g''(x) < 0$, thus

$$E_i''(t_k) = -f'(t_k) - [g'(\tilde{C}_i(t_k)) - g'(C(t_k))]\tilde{C}_i{}'(t_k) > 0,$$

which contradicts to the assumption that t_1 and t_2 are two consecutive zero points of $E'(t)$.

(iii) If $\tilde{C}_i{}'(T_i) > 0$, then $\tilde{C}_i{}'(t) > 0$ for all $t \in [T_i, \xi_i]$ by Lemma 2. As well, $C'(T_i) > 0$ considering that $E_i'(T_i) < 0$ as shown in (a), which further implies $C'(t) > 0$ for all $t \geq T_i$ by Lemma 2.

Assume there are more than one time points in $[T_i, \xi_i]$ at which $E_i(t)$ reach local minimum. Among these time points, we suppose t_1 is the smallest and t_2 is the largest. It is clear that $E_i'(t_1) = 0$, $E_i''(t_1) > 0$, $E_i'(t_2) = 0$, $E_i''(t_2) > 0$.

Now, we claim $t_2 = t_1$. If not, there must exist $t_3 \in (t_1, t_2)$ such that $E_i'(t) > 0$ for $t \in (t_1, t_3)$, $E_i'(t_3) = 0$ and $E_i''(t_3) < 0$.ss Thus, by developing the expression of $E_i''(t)$ at t_3, we have

$$E_i''(t_3) = -f'(t_3) - [g'(\tilde{C}_i(t_3)) - g'(C(t_3))][f(t_3) - g(C(t_3))] < 0. \tag{21}$$

We can observe that $g'(\tilde{C}_i(t_3)) - g'(C(t_3)) > 0$ since $g''(x) < 0$ and $C(t_3) > \tilde{C}_i(t_3)$. So, Eq. (21) leads to

$$f(t_3) + \frac{f'(t_3)}{g'(\tilde{C}_i(t_3)) - g'(C(t_3))} > g(C(t_3)). \tag{22}$$

At t_1, we have $E_i'(t_1) = 0$ and $E_i''(t_1) > 0$, the similar argument leads to

$$f(t_1) + \frac{f'(t_1)}{g'(\tilde{C}_i(t_1)) - g'(C(t_1))} < g(C(t_1)). \tag{23}$$

Moreover, since $g(C(t_3)) > g(C(t_1))$ given $C'(t) > 0$ for $t \in (t_1, t_3)$ and $g'(x) > 0$, we have

$$f(t_3) + \frac{f'(t_3)}{g'(\tilde{C}_i(t_3)) - g'(C(t_3))} > f(t_1) + \frac{f'(t_1)}{g'(\tilde{C}_i(t_1)) - g'(C(t_1))}. \tag{24}$$

Further, we have

$$g'(\tilde{C}_i(t_1)) - g'(C(t_1)) > g'(\tilde{C}_i(t_3)) - g'(C(t_3)) > 0. \tag{25}$$

This can be seen from the convexity of $g'(x)$ *w.r.t.* x as indicated by $g'''(x) > 0$. In fact, the convexity allows us to have

$$\frac{g'(C(t_1)) - g'(\tilde{C}_i(t_1))}{C(t_1) - \tilde{C}_i(t_1)} < \frac{g'(C(t_3)) - g'(\tilde{C}_i(t_3))}{C(t_3) - \tilde{C}_i(t_3)},$$

or

$$\frac{g'(\tilde{C}_i(t_1)) - g'(C(t_1))}{C(t_1) - \tilde{C}_i(t_1)} > \frac{g'(\tilde{C}_i(t_3)) - g'(C(t_3))}{C(t_3) - \tilde{C}_i(t_3)},$$

since $\tilde{C}_i(t_1) < \tilde{C}_i(t_3)$ and $C(t_1) < C(t_3)$. As $E_i'(t) > 0$ for $t \in (t_1, t_3)$, we have $\tilde{C}_i(t_1) - C(t_1) < \tilde{C}_i(t_3) - C(t_3) < 0$ that is equivalent to $C(t_1) - \tilde{C}_i(t_1) > C(t_3) - \tilde{C}_i(t_3) > 0$, which is used to affirm the inequality (Eq. (25)).

Using the fact $f'(t) < 0$ by Lemma 1, we have

$$f(t_1) + \frac{f'(t_1)}{g'(\tilde{C}_i(t_1)) - g'(C(t_1))} > f(t_1) + \frac{f'(t_1)}{g'(\tilde{C}_i(t_3)) - g'(C(t_3))}. \tag{26}$$

Now, let us consider the function $h(t) = f(t) + cf'(t)$ by denoting $c = 1/[g'(\tilde{C}_i(t_3)) - g'(C(t_3))]$. We have two important facts: 1. $h(t_3) > h(t_1)$; 2. $h'(t_3) < 0$. Fact 1 is the direct result of the two inequalities (Eq. (24), Eq. (26)).

As for Fact 2, we have

$$h'(t_3) = f'(t_3) + cf''(t_3) = f'(t_3) + \frac{c[f'(t_3)]^2}{f(t_3)} = \frac{f'(t_3)[f(t_3) + cf'(t_3)]}{f(t_3)}$$
$$= \frac{f'(t_3)h(t_3)}{f(t_3)} < 0, \tag{27}$$

using $f(t)f''(t) = [f'(t)]^2$ and $f'(t) < 0$ by Lemma 1 and $h(t_3) > 0$ by Eq. (22).

These two facts indicate there is a sign change of $h'(t)$ in the interval (t_1, t_3). Let t_4 be the largest time point in $[t_1, t_3)$ such that $h'(t_4) = 0$ and $h'(t) < 0$ for all $t \in (t_4, t_3]$. Especially, we have $h(t_4) > h(t_3) > 0$. However, if we repeat the similar argument as presented in the above inequality (Eq. (27)), we will have $h'(t_4) < 0$, which is clearly a contradiction. Therefore, the only possibility is $t_2 = t_1$, and we denote S_i^* by this unique local minimum time point. □

We now establish the key result on the global approximation error of Model (15) to Model (3).

Theorem 2 *For the solutions of the exact oral PK Model (3) and approximate PK Models (15), we denote by $E_{i,\max}$ the piecewise global maximum of $|E_i(t)|$ for $t \in [T_i, T_{i+1}]$, then*

$$E_{i,\max} = \max\{-E_i(S_i^*), E_i(T_{i+1})\},$$

where S_i^* is shown in Lemma 3. Moreover, $E_i(S_i^*)$ is determined by the negative root of the following quadratic equation

$$aE_i^2(S_i^*) + bE_i(S_i^*) + c = 0, \tag{28}$$

where

$$a = k_{el}(K_m + \tilde{C}_i(S_i^*)) > 0, \quad b = -\hat{g}(S_i^*)(K_m + \tilde{C}_i(S_i^*)) - k_{el}(K_m + \tilde{C}_i(S_i^*))^2 - V_{max}K_m,$$
$$c = -\hat{g}(S_i^*)(K_m + \tilde{C}_i(S_i^*))^2 < 0, \quad \hat{g}(S_i^*) = \frac{FD}{V_d}k_a\left(e^{-k_aS_i^*} - e^{-k_a\xi_i}\right) > 0. \tag{29}$$

Proof It directly follows from Lemma 3 that there exists a unique $S_i^* \in (T_i, \xi_i)$ such that $E_i(t)$ attains a global minimum for $t \in [T_i, \xi_i]$. It remains to investigate $E_i(t)$ for $t \in (\xi_i, T_{i+1}]$, where $E_i(t)$ obeys the following system

$$\begin{cases} E_i'(t) = (f(\xi_i) - f(t)) - [g(\tilde{C}_i(t)) - g(C(t))], & t \in (\xi_i, T_{i+1}], \\ E_i(\xi_i) = \tilde{C}_i(\xi_i) - C(\xi_i) < 0. \end{cases} \tag{30}$$

In fact, starting from ξ_i, $E_i(t)$ continues to increase as $E_i'(t) > 0$ from whence $E_i(t) \le 0$, which can be justified by $f'(t) < 0$ and $g'(x) > 0$. Now let us consider

the possibility that $E_i(t)$ arrives at zero at a certain time point $\eta_i < T_{i+1}$. For this circumstance, we will use the following inequality

$$g(\tilde{C}_i(t)) - g(C(t)) = g'(\bar{C}(t))E_i(t) = \left(k_{el} + \frac{V_{max}K_m}{(K_m + \bar{C}(t))^2}\right)E_i(t) < \left(k_{el} + \frac{V_{max}}{K_m}\right)E_i(t),$$

where $\bar{C}(t)$ is a value between $\tilde{C}_i(t)$ and $C(t)$ by Mean-Value Theorem. Accordingly, the dynamics of $E_i(t)$ satisfies

$$\begin{cases} E_i'(t) > (f(\xi_i) - f(\eta_i)) - \left(k_{el} + \frac{V_{max}}{K_m}\right)E_i(t), \ t \in (\eta_i, T_{i+1}], \\ E_i(\eta_i) = 0, \end{cases} \tag{31}$$

which indicates that $E_i(t)$ is monotonically increasing for all $t \in [\eta_i, T_{i+1}]$.

In the remaining part, we will show $\eta_i \in (\xi_i, T_{i+1})$ really exists. Otherwise, $E_i(t) < 0$, or we say $\tilde{C}_i(t) < C(t)$ for all $t \in [T_i, T_{i+1}]$. Taking integration from T_i to T_{i+1} of $E_i'(t)$ from Model (15) and Model (3), we can obtain

$$\begin{aligned} 0 &= \int_{T_i}^{T_{i+1}} \frac{FD}{V_d}k_a\left(e^{-k_a t} - e^{-k_a\xi_i}\right)dt \\ &= C(T_{i+1}) - \tilde{C}_i(T_{i+1}) + \int_{T_i}^{T_{i+1}} \left(\left(k_{el}C(t) + \frac{V_{max}C(t)}{K_m + C(t)}\right)\right. \\ &\quad \left. - \left(k_{el}\tilde{C}_i(t) + \frac{V_{max}\tilde{C}_i(t)}{K_m + \tilde{C}_i(t)}\right)\right)dt > 0, \end{aligned}$$

which leads to a contradiction.

Thus, the maximal absolute error $E_{i,\max}$ of $E_i(t)$ on the closed time interval $[T_i, T_{i+1}]$ is determined by the maximum value of $-E_i(S_i^*)$ and $E_i(T_{i+1})$.

For the convenience of calculation, the explicit formula of $E_i(S_i^*)$ can be given. $E_i'(S_i^*) = 0$ gives

$$\frac{FD}{V_d}k_a\left(e^{-k_a S_i^*} - e^{-k_a\xi_i}\right) = \left(k_{el}C(S_i^*) + \frac{V_{max}C(S_i^*)}{K_m + C(S_i^*)}\right) - \left(k_{el}\tilde{C}_i(S_i^*) + \frac{V_{max}\tilde{C}_i(S_i^*)}{K_m + \tilde{C}_i(S_i^*)}\right) \tag{32}$$

Replacing $C(S_i^*)$ by $\tilde{C}_i(S_i^*) - E_i(S_i^*)$ and rearranging Eq. (32) leads to a quadratic equation *w.r.t.* $E_i(S_i^*)$ as:

$$aE_i^2(S_i^*) + bE_i(S_i^*) + c = 0, \tag{33}$$

where a, b, c are defined in Eq. (29). Solving for $E_i(S_i^*)$, we have

$$E_i(S_i^*) = \frac{-b - \sqrt{b^2 - 4ac}}{2a}, \tag{34}$$

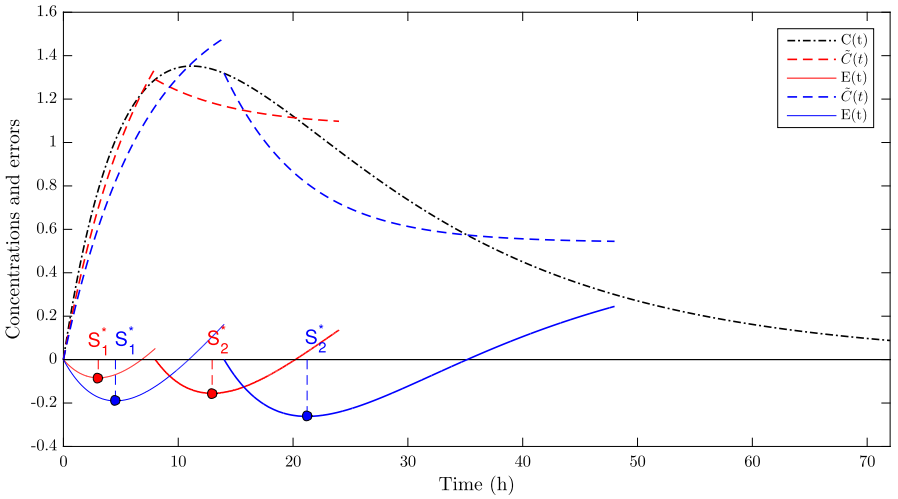

Fig. 1 (Color online) Illustration of the error function $E_i(t)$ of the proposed PK Model (15) to the exact oral Model (3), where $F = 1$; $k_a = 0.05\,h^{-1}$; $D = 350\,mg$; $V_d = 50\,L$; $V_{max} = 0.30\,mg/L/h$; $K_m = 5.3\,mg/L$; $k_{el} = 0.1\,h^{-1}$

where only the negative root of $E_i(S_i^*)$ is kept since $E_i(S_i^*) < 0$ is previously proved. This completes the proof. □

In Figure 1, we display two sets of concentration curves generated by the analytical solutions from Model (15) and their corresponding errors to the exact Model (3). It is noted, in each sampling-based time interval $[T_i, T_{i+1}]$, there exists a unique $S_i^* \in (T_i, T_{i+1})$ such that $E_i'(S_i^*) = 0$. Moreover $E_i(t)$ starts from zero, decreases to a negative local minimum, then back increases to a positive value at T_{i+1}. The illustration confirms our theoretical results proved in Theorem 2, and $E_{i,\max}$ can occur at either S_i^* or T_{i+1}.

If we consider the time range from 0 to infinity, we can base on well-chosen concentration samples from Model (3) to build a sequence of Model (15) with constant infusions, to uniformly approximate the exact solution of the former model.

Definition 3 For a given set of increasing time points $0 = T_0 < T_1 < T_2 < \ldots < T_n$, we define $\mathcal{T} = \{T_i\}_{i=0}^n$ by a sampling time scheme.

Theorem 3 *For any $\epsilon > 0$, we can find a sampling time scheme $\mathcal{T}_k$ consisting of a set of increasing times T_{i_k}, $i_k = 0, 1_k, \cdots, n_k$ such that $\sup_{t>0} |\tilde{C}^k(t) - C(t)| < \epsilon$. This also means that there exists a sequence of sampling time schemes $\{\mathcal{T}_k\}_{k=1}^\infty$ such that $\tilde{C}^k(t)$ uniformly converges to $C(t)$ for $t > 0$, i.e.,*

$$\lim_{k\to\infty} \sup_{t>0} |\tilde{C}^k(t) - C(t)| = 0.$$

Proof Given $\epsilon > 0$, we can find $T_{1_k} > 0$ such that $\sup_{0<t<T_{1_k}} |\tilde{C}^k(t) - C(t)| < \epsilon$. Then from T_{1_k}, and we can find $T_{2_k} > 0$ such that $\sup_{T_{1_k}<t<T_{2_k}} |\tilde{C}^k(t) - C(t)| < \epsilon$, etc. Since $\lim_{t\to\infty} C(t) = 0$, we can proceed to find a sufficiently large $T_{n_k} > 0$ such that $\sup_{t>T_{n_k}} |\tilde{C}^k(t) - C(t)| < \epsilon$ which ensures, for all $t > 0$, we have $|\tilde{C}^k(t) - C(t)| < \epsilon$. □

5 Numerical Simulations

Upon the theoretical basis provided by Theorems 2-3, we are able to obtain the analytical solution $\tilde{C}(t)$ from a sequence of PK sub-models (Model (15)) to approximate the exact solution $C(t)$ of Model (3).

5.1 Numerical Example

In all simulations, the following parameter values of Model (3) are fixed as

$$F = 1,\ D = 350\,mg,\ V_d = 50\,L,\ V_{max} = 0.30\,mg/L/h,\ K_m = 5.3\,mg/L.$$

Since our aim is to test the impact of different rates of absorption and elimination, as well as errors on the approximation between $\tilde{C}(t)$ and $C(t)$, we choose $k_a = 0.5, 0.1\,h^{-1}$, $k_{el} = 0.0434, 0.2\,h^{-1}$, and the allowable control error $\varepsilon = 0.05, 0.1, 0.2, 0.5$, respectively.

The simulation is performed over a time range of 0 to 120 hours, with $T_0 = 0$ and $\tilde{C}_0(0) = C(0) = 0$. The parameter ϵ is given a priori. First, we calculate the optimal sampling time scheme $\mathcal{T} = \{T_i\}_{i=0}^n$ through iteration. Then, we determine the associated constant infusion rates r_i of the PK sub-models (Eq. (14)). For convenience, a workflow illustrating how we can iteratively determine the optimal sampling time points, $\{T_i\}_{i=0}^{\infty}$, and the corresponding piecewise approximate of drug concentration time course, $\tilde{C}_i(t)$, is provided in Fig. 2. For each triplet ε, k_a and k_{el}, the calculated sampling time points T_i and constant infusion rates r_i are reported in Table 1. As we can observe, the larger the admissible error is, the fewer optimal sampling time points are needed.

Once the optimal sampling time points T_i and constant infusion rates r_i are determined, we are able to calculate the associated parameters C^{∞}, C_{β}^{∞}, q_1 and q_2, following Eqs. (8-9). For a specific example of $\varepsilon = 0.2$, $k_a = 0.5\,h^{-1}$ and $k_{el} = 0.0434\,h^{-1}$, the values of these parameters are reported in Table 2, which can be used to determine the required transcendental functions X_0 and Y_0.

Table 1 The optimal sampling time points (T_i) and corresponding constant infusion rates (r_i) for different admissible errors $\varepsilon = 0.05/0.1/0.2/0.5$ under different absorption and elimination scenarios of $k_a = 0.5/0.1\,h^{-1}$ and $k_{el} = 0.0434/0.2\,h^{-1}$. Other parameters are fixed as $F = 1$; $D = 350\,mg$; $V_d = 50\,L$; $V_{max} = 0.30\,mg/L/h$; $K_m = 5.3\,mg/L$.

ε	k_a	k_{el}	Optimal samplings T_i (Constant infusion rate r_i)							
0.05	0.5	0.0434	0 (3.0240)	0.6 (2.1880)	1.3 (1.5060)	2.1 (0.9640)	3.1 (0.5460)	4.4 (0.2500)	6.3 (0.0700)	9.9 (0.0004)
	0.1	0.0434	0 (0.6140)	2.7 (0.4600)	5.8 (0.3280)	9.5 (0.2180)	14.0 (0.1300)	19.9 (0.0640)	28.6 (0.0180)	46.2 (0.0010)
	0.1	0.2	0 (0.6080)	2.9 (0.4440)	6.3 (0.3040)	10.5 (0.1880)	16.0 (0.0960)	24.2 (0.0300)	41.3 (0.0014)	–
0.1	0.5	0.0434	0 (2.8840)	0.8 (1.8460)	1.8 (1.0460)	3.1 (0.4800)	5.0 (0.1300)	8.7 (0.0008)	–	–
	0.1	0.0434	0 (0.5760)	4.0 (0.3700)	9.0 (0.2080)	15.7 (0.0900)	26.2 (0.0160)	54.9 (0.0004)	–	–
	0.1	0.2	0 (0.5660)	4.4 (0.3420)	10.2 (0.1680)	19.1 (0.0440)	40.1 (0.0016)	–	–	–
0.2	0.5	0.0434	0 (2.6320)	1.2 (1.3220)	2.8 (0.4740)	5.5 (0.0400)	16.5 (0.0002)	–	–	–
	0.1	0.0434	0 (0.5260)	6.0 (0.2560)	14.7 (0.0780)	31.6 (0.0034)	–	–	–	–
	0.1	0.2	0 (0.5040)	7.0 (0.2020)	19.0 (0.0104)	–	–	–	–	–
0.5	0.5	0.0434	0 (2.2120)	2.0 (0.5480)	6.1 (0.0030)	–	–	–	–	–
	0.1	0.0434	0 (0.4220)	11.1 (0.0720)	42.0 (0.0014)	–	–	–	–	–
	0.1	0.2	0 (0.3640)	14.9 (0.0150)	–	–	–	–	–	–

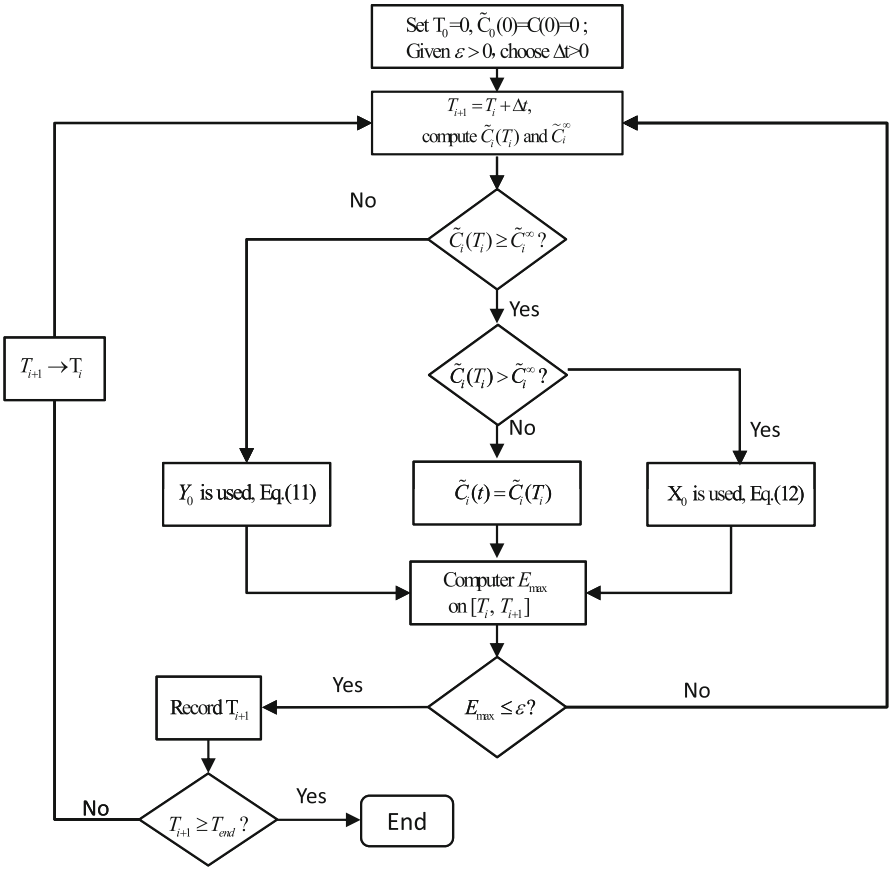

Fig. 2 The workflow for optimal sampling and deriving the closed-form approximate solution of Model (3)

Table 2 The computed parameter values which are required to express the analytical solution of Model (15) during each sampling time interval, where $\varepsilon = 0.2, k_a = 0.5\,h^{-1}, k_{el} = 0.0434\,h^{-1}, V_{max} = 0.3\,mg/L/h, K_m = 5.3\,mg/L, V_d = 50\,L, F = 1, D = 350\,mg$

$t \in [T_i, T_{i+1}]$	r_i	$\tilde{C}_i(T_i)$	$\tilde{C}^{\infty}$	$\tilde{C}_{\beta}^{\infty}$	q_1	q_2	X_0/Y_0
[0,1.2]	2.6320	0.0000	54.3469	5.9142	0.9898	0.0102	Y_0
[1.2,2.8]	1.3220	2.9892	24.7669	6.5185	0.9611	0.0389	Y_0
[2.8,5.5]	0.4740	4.6254	6.9901	8.2809	0.8048	0.1952	Y_0
[5.5,16.5]	0.0400	4.9382	0.4172	11.7080	0.4715	0.5285	X_0
[16.5,120]	0.0002	2.3312	0.0020	12.2098	0.4342	0.5658	X_0

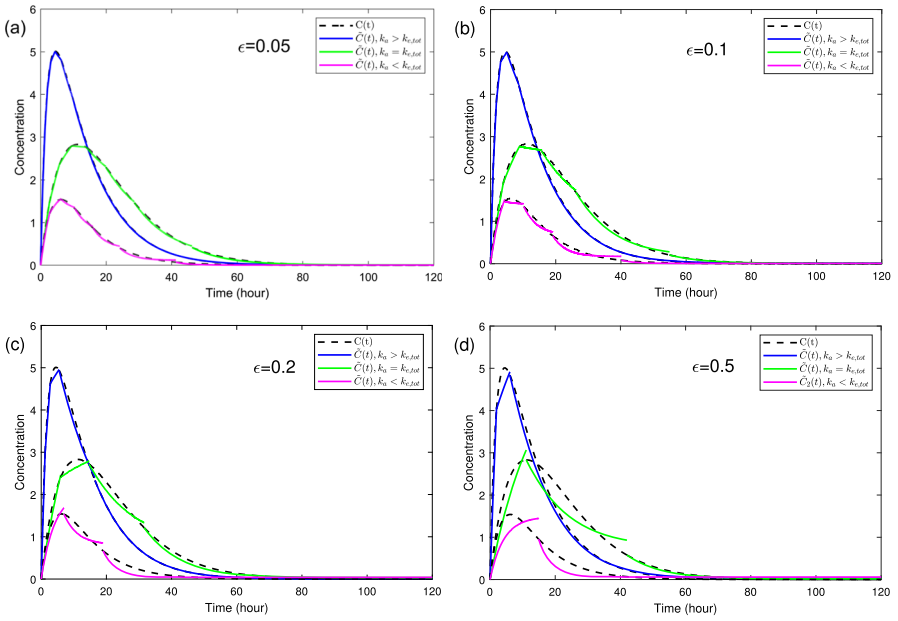

Fig. 3 (Color online) Illustration of $\tilde{C}(t)$ from a sequence of PK sub-models (15) to approximate the exact $C(t)$ from Model (3) with the allowable error $\varepsilon = 0.05, 0.1, 0.2, 0.5$. Blue solid line: $k_a > k_{e,tot} = k_{el} + V_{max}/K_m$ where $k_a = 0.5\,h^{-1}, k_{el} = 0.0434\,h^{-1}$; Green solid line: $k_a > k_{e,tot}$ where $k_a = 0.1\,h^{-1}$, $k_{el} = 0.0434\,h^{-1}$; Red solid line: $k_a < k_{e,tot}$ where $k_a = 0.1\,h^{-1}$, $k_{el} = 0.2\,h^{-1}$; Black dotted line: exact solution $C(t)$ of Model (3). Other parameter values are $F = 1$; $D = 350\,mg$; $V_d = 50\,L$; $V_{max} = 0.30\,mg/L/h$; $K_m = 5.3\,mg/L$.

Finally, we have

$$\tilde{C}(t) = \begin{cases} 54.3469 - 60.2611 \times Y_0(0.8817e^{-0.0434t}, 0.9898, 0.0102), & t \in [0, 1.2], \\ 24.7669 - 31.2854 \times Y_0(0.6740e^{-0.0434(t-1.2)}, 0.9611, 0.0389), & t \in [1.2, 2.8], \\ 6.9901 - 15.2711 \times Y_0(0.2157e^{-0.0434(t-2.8)}, 0.8048, 0.1952), & t \in [2.8, 5.5], \\ 0.4172 + 12.1252 \times X_0(0.7425e^{-0.0434(t-5.5)}, 0.4715, 0.5285), & t \in [5.5, 16.5], \\ 0.0020 + 12.2118 \times X_0(0.5377e^{-0.0434(t-16.5)}, 0.4342, 0.5658), & t \in [16.5, 120]. \end{cases} \quad (35)$$

For all triplets ε, k_a and k_{el} listed in Table 1, the corresponding curves of $\tilde{C}(t)$ and $C(t)$ are shown for comparison in Figure 3.

5.2 Local Adjustment

Sometimes, the approximation of peak concentration is especially deemed in practice, whereas it is not enough and impressive to use a single precision ϵ. An example is given in Fig. 3(d), where the approximation for $\varepsilon = 0.5$ could not virtually represent the peak concentration. In this case, we need to retouch the approximation by locally increasing the precision. That is to say, we can apply the same algorithm but reduce the ε value in a neighbourhood of the peak concentration. An example is illustrated in Figure 4, where we obtain a better local approximation by reducing ε from 0.5 to 0.1

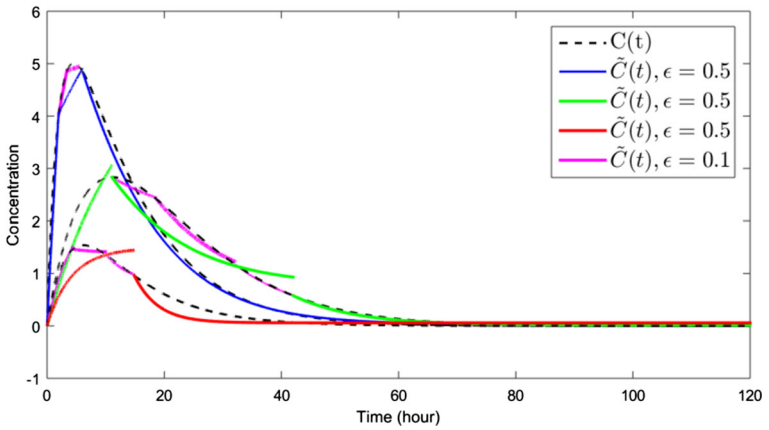

Fig. 4 (Color online) Illustration of a dense local approximation near the peak concentration by reducing ε from 0.5 to 0.1, where $F = 1$, $D = 350\,mg$, $V_d = 50\,L$, $k_a = 0.1\,h^{-1}$, $V_{max} = 0.3\,mg/L/h$, $K_m = 5.3\,mg/L$

in a time interval around the peak time. Other special requirements can be similarly implemented.

5.3 Robustness in Presence of Variability

Up till now, we have not taken into account the presence of uncertainty in Model (3). For this, we can simulate more realistic situations by adding randomness to the simulated concentrations of Model (3) and check the robustness of our proposed sampling-based approximation algorithm. First, we assume to use 14 drug plasma sampling points 0.1, 0.5, 1, 1.5, 2, 3, 4, 6, 8, 12, 18, 24, 36, 48h, we obtain the corresponding concentrations: 0.33, 1.48, 2.58, 3.38, 3.96, 4.62, 4.88, 4.76, 4.30, 3.26, 2.01, 1.19, 0.39, $0.12\,mg/L$ from Model (3) using the model parameters shown in Fig. 4 and ODE45 solver in MATLAB. Suppose the real concentrations are log-normally distributed around the deterministic concentration of Model (3) at anytime, i.e., $\ln(C_{real}(t)) \sim \mathcal{N}(\ln C(t), \sigma^2)$, we thus simulate $N = 100$ PK profiles with each consisting of 14 'real' concentration data. In the next step, we refit each set of 14 'real' concentration data with the least square method to obtain the corresponding model parameters for N numerical oral models. Accordingly, we obtain N piecewise approximate analytical drug concentrations $\tilde{C}_j(t)$ $(j = 1, 2, \cdots, N)$ by applying the proposed algorithm. Finally, the robustness of our proposed approximation algorithm regarding variability in concentration is evaluated using the following Mean Error index

$$\mathrm{ME} = \frac{1}{14N} \sum_{j=1}^{N} \sum_{k=1}^{14} \left| C(t_k) - \tilde{C}_j(t_k) \right|, \tag{36}$$

where t_k $(k = 1, 2, \cdots, 14)$ are the above time points.

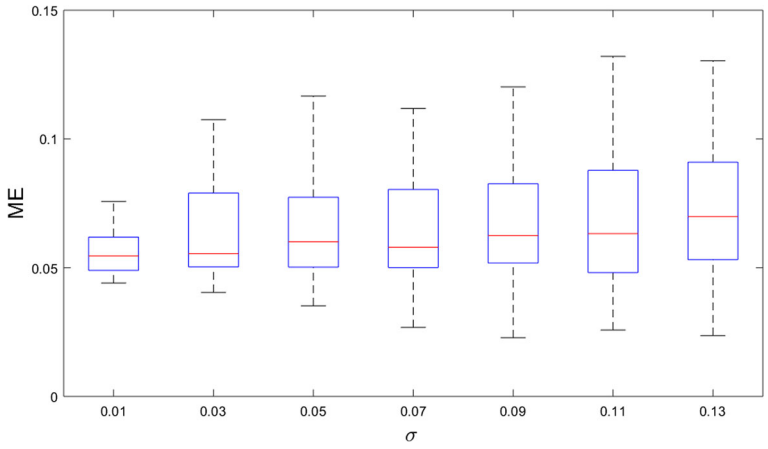

Fig. 5 (Color online) Robustness test in the presence of variability by displaying mean errors with respect to σ after 100 simulations

The result is shown in Figure 5. As we can observe, the approximation is quite robust despite the gradual increase of Mean Error as the standard deviation σ increases.

6 Discussion and Conclusion

In this paper, we have studied, in the case of the first-order absorption, the solution of one-compartment PK model with the simultaneous first-order and Michaelis-Menten elimination. Different to the cases of bolus or constant infusion that we previously studied [13, 14], the time-varying absorption intertwines with the nonlinear elimination in such a way as to separate them is impossible. For this reason, we cannot expect an exact analytical solution to Model (3). However the popularity and importance of oral drugs bearing the first-order absorption and the nonlinear elimination properties draw our attention to the mathematical expression of their pharmacokinetics, and the analytical solution to approximate Model (3) within a controlled precision seems a reasonable strategy that is worthy to further mathematical studies.

Different to other non-mechanistic approximations such as the polynomial or spline functions, this study clearly brings the advantage of maintaining meaningful pharmacokinetic characteristics in the approximation process. That is, the proposed PK sub-models have the same distribution/elimination kinetics, and absorbed dose amount in the associated time scheme remains the same as the original Model (3), whereas the drug administration route is altered to the constant infusion since its analytical solution is mathematically available.

Indeed, we have developed and demonstrated a unified scheme capable of efficiently determining the explicit expression of drug concentration over time for Model (3) under a global unified measurement constraint (see Theorem 3). Furthermore, numerical simulations were conducted to validate the feasibility of deriving explicit curves of drug concentration over time from the explicit expressions of PK sub-models (15),

considering various rates of absorption (k_a) and elimination (k_{el}), as well as differing approximation accuracies (ε).

As shown in Fig. 3, smaller precision values (ε) lead to more accurate approximations. Additionally, achieving the desired precision requires only a small number of samplings. For example, when $k_a = 0.1$ and $k_{el} = 0.2$, reducing ε from 0.5 to 0.2, 0.1, and 0.05 results in the least number of samplings changing from 1 to 2, 4, and 6, respectively, which is highly practical in clinical settings.

It is important to emphasize that, in order to touch the peak concentration, C_{max}, our algorithm can be further improved for the decision on T_i by incorporating additional practical considerations, as illustrated in Fig. 4. Such refinements are fully compatible with our approach.

Moreover, the proposed method for deriving approximate analytical solutions is both more efficient and more direct compared to existing pharmacokinetic studies, such as [19], which only established upper and lower bounds for drug concentration and required a large number of samples to achieve satisfactory global convergence.

The challenge of the current work is to demonstrate the theoretical feasibility for the approximate error between the solution of the sequence of constant infusion models and the exact one of the oral model (see Theorem 2). This is the cornerstone for a reliable algorithm that guarantees the computability of the approximation and the subsequent simulations. To resume, the key step is to prove the uniqueness of the intersection point of $C'(t)$ and $\tilde{C}'(t)$ on each time interval. However, since two convex/concave functions may intersect on more than one point, the problem becomes complicated for the case when both $C'(t)$ and $\tilde{C}_i(t)$ are strictly decreasing and strictly concave up. Though lack of mathematical theory that is readily available, we have developed several techniques directly on the specified properties of the absorption and elimination of the studied model, which finally help to confirm the uniqueness of the local minimum $E(S_i^*)$ on the open interval (T_i, T_{i+1}). However, we still believe that the current condition can be relaxed for more general models in the future.

As we mentioned in the introduction, the nonlinearity discussed in the paper is largely present in biologics. The precision of the characterization of their pharmacokinetics has become a major issue concerning their efficacy and safety, whereas this is the facility of the analytical solution in terms of mechanistic description and explanation. Our proposed mechanistic '*model-to-model*' approach provides a novel mathematical solution to difficult issues when more complicated components are involved in a drug's administration, disposition, metabolism and excretion (ADME), such as the first-oral administration discussed in this paper. However, our work is limited to the strategy of using a sequence of constant infusion models to approximate the exact oral model. Since it is based on equal dose administration on each time interval, the approximation is not continuous but disjointed on several time points. This problem maybe solved by introducing mixed administration of both intravenous bolus and infusion administrations, or even changing the condition of equal dose to equal exposure, or including other specific pharmacological concerns. Moreover, since it is the analytical approximation strategy that we adopted here for solution, the methodology can extend to more complex cases such as more than one-compartment pharmacokinetic models. We leave all these in our future investigation.

Acknowledgements The work is supported by National Natural Science Foundation of China (Nos. 12271346 and 12071300), Natural Sciences and Engineering Research Council of Canada, and Le Fonds de recherche du Québec-Nature et technologies (FRQNT). The authors would like to thank Min Chen for the technical support in simulations and Prof. Lan Zou for the valuable discussion, and two anonymous reviewers for their helpful and insightful comments which lead to the high improvement of the article's quality.

Declarations

Competing Interest The authors declare that they have no competing of interests.

Data Availability Statement No data was used for the research described in the article.

References

1. Ahmad, Y.A., David, J.R.F., Richard, N.U.: ADVAN-style analytical solutions for common pharmacokinetic models. J Pharmacol Tox Met. **73**, 42–48 (2015)
2. Beguerisse-Díaz, M., Desikan, R., Barahona, M.: Linear models of activation cascades: analytical solutions and coarsegraining of delayed signal transduction. J. R. Soc. Interface **13**, 20160409 (2016)
3. Bertrand, J., Mentré, F.: Mathematical expressions of the pharmacokinetic and pharmacodynamic models implemented in the monolix software. Paris Diderot University, Paris (2008)
4. D'Argenio, D.Z., Bae, K.S.: Analytical solution of linear multi-compartment models with non-zero initial condition and its implementation with R. Transl Clin Pharmacol. **27**(2), 43–51 (2019)
5. Hof, F., Bridge, L.J.: Exact solutions and equi-dosing regimen regions for multi-dose pharmacokinetics models with transit compartments. J. Pharmacokinet Pharmacodyn. **48**, 99–131 (2021)
6. Saganuwan, S.A.: Application of modified Michaelis-Menten equations for determination of enzyme inducing and inhibiting drugs. BMC Pharmacol. Toxicol. **22**, 57 (2021)
7. Morales-Delgado, V.F., Taneco-Hern ández, M.A., Vargas-De-León, C., Gómez-Aguilar, J.F.: Exact solutions to fractional pharmacokinetic models using multivariate Mittag-Leffler functions, Chaos. Solitons & Fractals **168**, 113164 (2023)
8. Tang, S., Xiao, Y.: One-compartment model with Michaelis-Menten elimination kinetics and therapeutic window: an analytical approach. J. Pharmacokinet Pharmacodyn. **34**, 807–827 (2007)
9. Sopasakis, P., Sarimveis, H., Macheras, P., Dokoumetzidis, A.: Fractional calculus in pharmacokinetics. J. Pharmacokinet Pharmacodyn. **45**, 107–125 (2018)
10. Sorzano, C.O.S., Moreno, M.A.P., Vilas, J.L.: An Analytical Solution for Saturable Absorption in Pharmacokinetics Models. Pharm. Res. **40**(2), 481–485 (2023)
11. Shi, S.: Biologics: an update and challenge of their pharmacokinetics. Curr. Drug Metab. **15**(3), 271–290 (2014)
12. Ludden, T.M.: Nonlinear pharmacokinetics: clinical Implications. Clin. Pharmacokinet. **20**(6), 429–446 (1991)
13. Wu, X., Li, J., Nekka, F.: Closed form solutions and dominant elimination pathways of simultaneous first-order and Michaelis-Menten kinetics. J. Pharmacokinet Pharmacodyn. **42**, 151–161 (2015)
14. Wu, X., Chen, M., Li, J.: Constant infusion case of one compartment pharmacokinetic model with simultaneous first-order and Michaelis-Menten elimination: Analytical solution and drug exposure formula. J. Pharmacokinet Pharmacodyn. **48**, 495–508 (2021)
15. Kim, J., De Jesus, O.: StatPearls. StatPearls Publishing; Treasure Island (FL): Medication Routes of Administration (2024)
16. Poyatos, L., Pérez-Acevedo, A.P., Papaseit, E., et al.: Oral Administration of Cannabis and *Delta*-9-tetrahydrocannabinol (THC) Preparations: A Systematic Review. Medicina (Kaunas) **56**(6), 309 (2020)
17. Adepu, S., Ramakrishna, S.: Controlled drug delivery systems: current status and future directions. Molecules **26**(19), 5905 (2021)
18. Wu, X., Li, J.: Morphism classification of a family of transcendent functions arising from pharmacokinetic modelling. Math Meth Appl Sci. **44**, 140–152 (2021)

19. Hu, X., Tang, S.: Approximate solutions to the nonlinear compartmental model for extravascular administration. Appl. Math. Mech. **35**(9), 1033–1045 (2014)